

This paper reports the results of the physical and numerical experiments on determining the stressed-strained state of concrete in protective structures in the region of the effect of local point laser radiation. The software package LIRA10.8 (release 3.4) was used to build a computer model in the statement of a stationary thermal conductivity problem. To this end, the findings from the experimental studies were applied – the resulting temperature distribution and changes in the structure of concrete on the surface and deep into concrete cubes for more than 120 samples of concrete with three levels of moisture content: dried, natural humidity, and water-saturated. This paper gives the parameters of the simulation, the results of a numerical experiment, their analysis, and comparison with the results of a physical experiment.

The temperature fields when establishing the dynamic temperature equilibrium, the level of stresses in concrete, derived from the physical experiments, correlate well with the results of the numerical experiment. The maximum temperature determined by the optical method at the surface of concrete was $1,350+50$ °C. Deviations at control points do not exceed $12-70$ °C in the temperature effect zone and $18-176$ °C ($1-11$ %). At the rated radiation power of 30 W, the second stage of interaction was achieved; at 100 W – the fourth stage for concrete with a moisture content of 0–2.5 %; and, for water-saturated concrete, the fifth stage of interaction with the laser beam. A significant decrease in the thresholds between the stages of interaction between laser radiation and concrete was revealed, especially water-saturated concrete, compared to the thresholds for metals (the thresholds between the third and fifth stages were reduced by 10^3-10^4 times). The destruction of the walls of water-saturated pores in concrete occurred under the pressure of water vapor. The tangent stresses, in this case, were 1.7 MPa, and the values for the coefficient K_p , determined by the method of acoustic emission, were in the range of 4–6. Such results explain the absence of normal microcracks due to the hoop effect.

It was established that in the contact zone between a laser beam and concrete, about 90 % of the radiation energy dissipates, and in the adjacent heating zone – up to 77 %. The optimal speed of beam movement when cleaning the concrete surface from organic, paint, and other types of contamination of 0.5–2 mm/s (surface temperature, 100–300 °C) has been proposed

Keywords: heavy concrete, moisture content, laser radiation, protective properties

UDC 624.042.7:624.21:625.71(075.8)

DOI: 10.15587/1729-4061.2021.232671

DETERMINING THE STRESSED- STRAINED STATE OF CONCRETE IN THE ZONE OF EXPOSURE TO LOCAL LASER RADIATION

Ihor Karkhut

Corresponding author

PhD, Associate Professor

Department of Building

Constructions and Bridges

Lviv Polytechnic National University

S. Bandery str., 12, Lviv,

Ukraine, 79013

E-mail: Karkhoot1@gmail.com

Received date 24.03.2021

Accepted date 18.05.2021

Published date 30.06.2021

How to Cite: Karkhut, I. (2021). Determining the stressed-strained state of concrete in the zone of exposure to local laser radiation. *Eastern-European Journal of Enterprise Technologies*, 3 (7 (111)), 24–36.doi: <https://doi.org/10.15587/1729-4061.2021.232671>

1. Introduction

The interaction between laser radiation and the surface of metals, including phase transformations, has been studied in detail, which made it possible to widely introduce it into the machining processes. Lasers with radiation power up to 10^{16} W/cm² allow the widespread use of various technological operations with materials. The application of lasers has significant advantages over traditional ones: the ability to process miniature parts without contact with the tool, the high accuracy of laser impact, the possibility to pass through transparent shells. Lasers also provide the lightness and speed of beam movement in space, the automation and safety of machining operations, the high durability of parts after processing, better working conditions, and the culture of manufacturing. In addition, high energy makes it possible to quickly change the material's SSS, typically towards the growth of stresses due to the evolution of temperature deformations. Melting and evaporation in the contact area with laser radiation cause mechanical destruction, including due to temperature stresses. With a pulse transfer of energy, it is absorbed at the surface of the material, thereby heating the material, with temperature destruction in the contact area

between the beam and material, the products of destruction from the contact surface are released, cooling follows the pulse termination. The transience of these processes allows them to be considered thermo-elastic, which particularly accurately describes the heating of glass, silts, ceramics. The rate of increase in temperature stresses and the growth of cracks depend on the heat transfer mechanism in the material.

These technological processes involving high temperatures are common in various industries (energy, metallurgy, chemical and glass industry, ceramic materials enterprises, galvanic production, etc.). That predetermines the need to study the processes of interaction between temperature carriers in their local contact with the structures at industrial enterprise facilities in order to improve the reliability of design, in particular, calculations of strength and deformability. In many countries, studies are being carried out into the effect of laser radiation on the surface of other building materials, such as brick, gypsum, and cellular concrete. They would allow for a wider introduction of such modern technologies in the construction industry. It is also important to study the behavior of concrete in protective reinforced concrete structures under a local high-temperature impact.

2. Literature review and problem statement

Numerous studies into the thermal effect of radiation on the surface of solids confirm the possibility of applying a laser to machining various materials. In particular, paper [1] reports the results of investigating a local effect of laser heating on the surface of metals (effect on the surface limited by a spot of the beam), which leads to the appearance of three-dimensional temperature fields and its short duration. Depending on the density of radiation power and the duration of its action on the material during the interaction between laser radiation and a substance, the following five stages have been defined:

1. The fall and partial reflection of radiation, $q > 0$.
2. Absorption and heating, $q < 10^2 \text{ W/cm}^2$.
3. Melting, $q = 10^5 \text{ W/cm}^2$.
4. Erosion, $q = 10^5 - 10^8 \text{ W/cm}^2$.
5. Plasma formation, $q > 10^7 \text{ W/cm}^2$.

The effect on composite materials was not investigated, it was not established whether their plastic properties appear. The impact of the moisture content in materials and the effect of water evaporation on the propagation of temperature fields were not considered.

Work [2] considered the issues of thermodynamics and the theory of heat transfer in high-temperature processes. It focuses on the melting processes of metals and their application for cutting and finishing surfaces. The great possibilities of using laser technologies in construction are indicated in paper [3]. It is indicated that there are almost no studies into the thermodynamic behavior of composite materials, which include heavy concrete, under the influence of local high-temperature laser radiation.

The evolution of cracks and the gradient of stresses under a local temperature load is limited to the compression zones (the hoop effect) in the material. Paper [4] tackles the modeling of these processes. It considers the model of semi-finite space to be correct. The cited study takes into consideration a change in the intensity of pulses of laser radiation over time. The duration of pulses from gas and ruby lasers is 0.1–1.0 ms. With a small thickness of the heated layer, the process was modeled in the form of a surface heat source, solving a one-dimensional heat conductivity problem for semi-finite space. To this end, one needs to know the specific power or heat flow of the beam. The effectiveness of such a source depends on the shape of the distribution of its power. Work [4] describes the Gaussian and uniform distribution models; it is established that the ratio of maximum temperatures in those distributions does not depend on the radius of the source. Such properties of the temperature field as the heating rate, the depth of the heated layer of the material were not studied in detail. Only the thickness of the hardened layer in metals was established and the maximum temperature in the area of the beam spot and the corresponding effective depth of heating, including the depth of erosion for stages I–IV of interaction, were localized.

Works [5, 6] report the results of studying the interaction between laser radiation and the surface of ceramic bricks and gypsum composites. In particular, the results showed the possibility of using laser radiation to strengthen the old damaged masonry of brick walls and protect architectural monuments against adverse environmental impact. For protective reinforced concrete structures, investigating the influence of a local high-temperature load under an emergency mode is also of great importance. Proper and more accurate

consideration of the impact of the thermal shock and local heating on load-bearing structures, in this case, reinforced concrete, makes it possible to improve reliability, gain an economic effect in the design and construction of protective structures. The peculiarities of the processes of interaction of laser radiation with structural concrete, which is a composite material, were not investigated.

Paper [7] reports the results of studying the effect of laser radiation on cellular concrete and the peculiarities of the interaction of radiation with this material at different levels of moisture content. The coefficients of thermal conductivity of cellular concrete at different levels of moisture content were studied. The issue of interaction and the possibility for the laser radiation to machine the surface of such material as structural heavy concrete was addressed in work [8]. It is indicated that a decrease in the thermal conductivity and heat capacity of concrete leads to an increase in temperature difference between the heated and non-heated sections of concrete. In case of repeated thermal shocks, there is a gradual destruction of concrete, which can lead to a decrease in the protective layer of concrete, the height of the compressed zone, the design cross-section, etc. Therefore, when determining the type, composition, operating conditions of concrete in load-bearing protective structures, one must take into account this feature.

The issue of the impact of concrete moisture content on treatment processes remains unattended in work [8]. Under actual operating conditions, the moisture content of concrete varies depending on the climatic zone, the time of year, the presence of insulation, indoor conditions, and other random factors. Therefore, the need to study the effect of drying, water saturation, and the natural level of moisture content on the interaction of laser radiation with concrete is indisputable.

The possibility of removing dirt from the surface of concrete was considered in work [9]. At the same time, it is necessary to clarify the speed of movement of the beam on the surface of concrete to prevent the appearance of microcracks and melting of concrete components. The level of stresses in concrete, the nature of crack formation processes in the zone of interaction with laser radiation can be determined by an acoustic-emission method [10, 11]. Applying the acoustic emission method makes it possible to determine the level of the K_p coefficient in real time, to control the process of microcracking. No experimental studies using the method of acoustic-emission control of crack formation in concrete in the contact zone with laser radiation were found.

Work [12] reports the results of studying the processes taking place in concrete during its destruction into depth using laser heating. The possibility of making cavities and holes in concrete samples up to 20 mm thick due to erosion (the fourth stage of interaction) has been experimentally proven with a laser with a rated capacity of 1.6 kW. At the same time, for the rapid removal of the destruction products under the action of gravity, it is recommended to perform the machining from the bottom up. No analysis of the effect of moisture content on the processes of erosion destruction of concrete was carried out.

Paper [13] established the optimal speed of concrete surface machining to form a vitreous layer. A stable vitreous layer was formed at a surface machining rate of 480 mm/min (8 mm/s). The main source of porous structures on the contact surface, according to the authors, is CO_2 that forms during the destruction of cement stone components. The presence of water in the

pores of concrete and its effect on the formation of a porous layer and, accordingly, the strength of contact between the vitreous layer and the substrate were not taken into consideration.

The possible impact of the presence of water in the pores of cement stone on a decrease in the rate of heating of the surface under the action of laser radiation was noted in work [14]. It is indicated that more thorough conclusions need additional research.

Given the large volumes and long service life of reinforced concrete structures, it is also of great interest to investigate the rate of heating a concrete surface and the depth of the heated layer, which determine its protective properties, including the influence of a moisture content level. This factor is very important for recessed protective structures, whose outer layers of concrete are often in a water-saturated state.

3. The aim and objectives of the study

The aim of this study is to determine patterns of change in the stressed-strained state of concrete in the area of interaction with laser radiation. That would make it possible to properly take into consideration such influences when devising technological processes for machining concrete surfaces and designing the reinforced concrete structures for protective facilities.

To achieve the set aim, the following tasks have been solved:

- to investigate the stressed-strained state in the vicinity of the action of a point temperature effect on heavy concrete, to determine the level of stresses in concrete;
- to investigate temperature fields at the surface and deep into concrete and determine the time of establishing a dynamic temperature equilibrium and the features of phase transitions;
- to develop a computer model of interaction between laser radiation and heavy concrete;
- to establish working parameters for the technology of machining the surface of concrete by laser radiation.

4. Materials and methods to study concrete under the action of local laser radiation

The stressed-strained state of concrete was studied by conducting a numerical experiment. The stationary thermal conductivity problem was stated with the help of LIRA10.8 software package (release 3.4).

The temperatures in the nodes of the finite elements, derived from the calculation, were compared with those acquired during experimental studies. The levels of stresses in concrete were assessed at the fifth minute of heating (the time of the dynamic stabilization of temperature fields).

The heat flow was simulated at five levels (100 W; 77 W; 50 W; 27 W; 10 W) of the laser's rated power.

That has made it possible to estimate the share of the power spent on heating the samples. The effect was then determined on temperature distribution and the stressed-strained state of concrete at the rated power of the laser of 1,000 W; 770 W; 500 W; 270 W, and 100 W (with full energy transmission without dissipation).

At the same time, the simulated power of the laser was supposed to provide such temperature on the surface of the

contour at which the process of “cold plasma” combustion took place (Fig. 1).



Fig. 1. The fifth stage of interaction of laser radiation with concrete (plasma is burning at the surface)

The temperature in this zone, registered by CA thermocouples and a visual pyrometer exceeded 1,300 °C, which is higher than the temperature of destruction of concrete at 600–750 °C. Therefore, it was very important to properly simulate the contact and intermediate layers between the surface upon which the beam arrived and the concrete itself.

The surface contact layer of vitreous material formed during the fusion of cement stone and quartz sand is very close to aporite glass. The chemical structure of this glass, $\text{CaO} \cdot \text{Al}_2\text{O}_3 \cdot 2\text{SiO}_2$, is closest to the chemical composition of the starting materials in a high-temperature impact zone (Portland cement and sand).

The thickness of this layer, determined by the results of experimental studies, was on average statistically about 1 mm. For this material, the thermal conductivity coefficient of 0.11 W/m°C is known. The dependence of the thermal conductivity coefficient of this layer on changes in temperature was neglected since at the interface with an intermediate porous layer the thermal conductivity was considered constant. An intermediate porous layer, formed from the products of destruction of cement stone and quartz sand in the experimental studies, was also registered with an average thickness of 1 mm. The pores in this layer were close to the pore sizes in insulating foam-concrete of medium density, 300 kg/m³, with a thermal conductivity coefficient of 0.08 W/m °C.

To study the temperature fields in concrete at local point heating, several series of experiments were carried out. The experiments involved conventional heavy concretes of three classes at compression strength C12/15, C20/25, C30/35. Cubes with a 100- and 150-mm edge were accepted as the samples of series I. The next two series employed cubes with a 100-mm edge.

Standard heavy concrete on the Portland cement was chosen for the study taking into consideration the peculiarities of the thermal shock and subsequent local heating, as the heat-resistant concrete demonstrates an increase in the effect of a thermal shock. In addition, 95 % of the structures of all protective facilities are made from regular heavy concrete.

The cubes from series I were concreted according to factory technology at the bench for the manufacture of round-hollow slabs at Lviv plant ZBV No. 1 and aged in the laboratory NDL-23 at the BCM Department, NU “Lviv Polytechnic”, over 1–70 months before the tests.

The cubes of series II or series III were concreted in the laboratory NDL-23. Storage conditions met the requirements set in [15, 16]. The materials and their consumption

per 1 m³ of concrete for cubes of series I are given in Table 1, for series II and series III – in Tables 2, 3.

Series II was made of concrete, plasticized with the admixture Stachment F+. The cubes from series III were produced at W/C=0.2–0.22 (the minimum amount of free water in the pores) with an admixture based on polycarboxylates. According to the program, three series of samples with 96 pieces of each class of concrete in each series were produced. The moisture content impact was assessed by comparing the strength of the cubes of three levels of relative humidity: 0 % (dried samples), 0.2–1 % (samples with a natural moisture content “n/h”) and 2.5–7.3 % (water-saturated “w/s” samples) during local laser heating.

Table 1

Materials selected for the manufacture of samples from series I

Material	Origin	Consumption for the grade of concrete, kg/m ³		
		C12/15	C20/25	C30/35
Cement	IFC-400	320	420	520
Sand	Trostyanyets quarry	400	400	500
Rubble 5–20	Klesivsky quarry	1250	1250	1250
Water	Tap	160	210	260

Table 2

Materials selected for the manufacture of samples from series II

Material	Origin	Consumption for the grade of concrete, kg/m ³		
		C12/15	C20/25	C30/35
Cement	IFC-400	250	420	520
Sand	Trostyanyets quarry	915	595	410
Rubble 5–20	Klesivsky quarry	1,250	1,250	1,250
Water	Tap	100	165	200
Admixture	Stachment F+	3.0	5.04	6.24

Table 3

Materials selected for the manufacture of samples from series III

Material	Origin	Consumption for the grade of concrete, kg/m ³		
		C12/15	C20/25	C30/35
Cement	IFC-400	320	420	520
Sand	Trostyanyets quarry	930	790	660
Rubble 5–20	Klesivsky quarry	1,250	1,250	1,250
Water	Tap	70	90	105
Admixture	Stachment-2000	3.2	4.2	5.2

At the age of 28 days, part of the cubes was tested to determine the strength at single-axial compression, some were saturated with water and dried according to the procedure from [11]. In this case, the samples were weighed with

an accuracy of 2 g to determine the volumetric weight and humidity. Weighing of samples was carried out at the age of three days, up to six years before the force and thermal force tests (Table 4).

Table 4

Density of concrete cubes (average of two samples), kg/m³

Series No.	Concrete class	Storage conditions	Age at testing, (day), month						
			(3)	1	3	6	12	49	70
1	C12/15	dried	–	2,240	2,242	2,240	2,245	2,245	2,237
		n/h	2,298	2,258	2,254	2,252	2,250	2,250	2,254
		w/s	–	2,301	2,304	2,303	2,305	2,300	2,305
	C20/25	dried	–	2,279	2,280	2,281	2,280	2,280	–
		n/h	2,308	2,300	2,295	2,293	2,291	2,290	–
		w/s	–	2,336	2,338	2,342	2,340	2,440	–
	C30/35	dried	–	2,352	2,350	2,349	2,352	2,352	–
		n/h	2,388	2,374	2,360	2,366	2,364	2,366	–
		w/s	–	2,418	2,421	2,422	2,419	2,420	–
2	C12/15	dried	–	2,184	2,188	2,190	2,185	2,188	–
		n/h	2,315	2,298	2,294	2,291	2,290	2,291	–
		w/s	–	2,339	2,344	2,341	2,345	2,346	–
	C20/25	dried	–	2,310	2,311	2,317	2,312	2,315	2,327
		n/h	2,346	2,324	2,321	2,320	2,319	2,320	2,338
		w/s	–	2,364	2,364	2,366	2,365	2,365	2,356
	C30/35	dried	–	2,365	2,370	2,370	2,370	2,372	–
		n/h	2,436	2,374	2,374	2,372	2,373	2,374	–
		w/s	–	2,409	2,410	2,408	2,410	2,410	–
3	C12/15	dried	–	2,297	2,295	2,292	2,290	2,290	–
		n/h	2,357	2,322	2,317	2,314	2,311	2,250	–
		w/s	–	2,363	2,368	2,370	2,367	2,370	–
	C20/25	dried	–	2,396	2,395	2,402	2,403	2,405	–
		n/h	2,414	2,410	2,408	2,406	2,405	2,400	–
		w/s	–	2,453	2,505	2,507	2,504	2,502	–
	C30/35	dried	–	2,486	2,490	2,493	2,488	2,490	2,464
		n/h	2,506	2,500	2,498	2,497	2,496	2,506	2,474
		w/s	–	2,536	2,586	2,590	2,585	2,520	2,495

Two cubes of each level of moisture content were tested for laser radiation. Moisture content mainly affects the speed of propagation of the evaporation front and the growth of intraporal pressure, so it was also determined for concrete samples. Concrete was heated by gas lasers with a power of 30 W (series I, LGN-703 laser, 3–5 min irradiation) and 100 W (series II and series III, ILGN-709 laser) with a radiation wavelength of 10.6 μm. When using a laser with a power of 30 W, only the second stage of interaction was achieved – the heating and evaporation of moisture from the pores of concrete, so a more powerful laser was used in further studies.

For comparative analysis, some of the samples were tested during the joint action of single-axial compression under the press P-125 and a laser temperature load immediately after stabilizing the temperature field, which lasted over 4–5 minutes. The initial load level for laser heating was set within 0.3f_{cm,cube} – microcracking, 0.65f_{cm,cube} – operational load, and 0.95f_{cm,cube} – the state close to the maximum bearing capacity. The cubes were also tested to determine the class of concrete and strength at the age of 3, 6, 12, 49, and 70 months without heating.

Stable indicators during the thermal force experiments involving series II and III were the intensity of radiation – up

to 10^3 W/cm^2 . The distance to the source was 0.5 m (when testing series I, a distance of 0.3 m), and the radiation time was 5 minutes.

The heating point was in the geometric center of the face of the cube. The heating covered an area of $0.38\text{--}0.45 \text{ cm}^2$ (the area of the spot of interaction between the laser beam and the surface of a concrete cube). At the same time, every 10 s, in real time, the multichannel thermometer TT-C101M registered the heating temperature with an accuracy of 3°C to determine the shape of the temperature field. The temperature was measured by CA thermocouples glued to the surface of the heated cube, along two coordinate axes in increments of 2.5 mm, and in the depth of samples.

Additionally, a pyrometer and a digital heat scanner with a temperature range of $0\text{--}450^\circ\text{C}$ were used to control in real time the process of heating the surface of the cube (Fig. 2). The heat scanner software made it possible to build temperature change charts in each cell (Fig. 4).

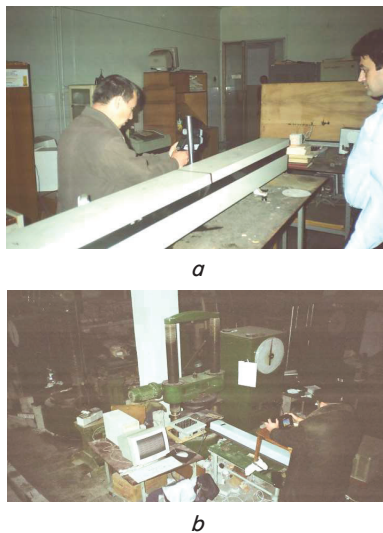


Fig. 2. Controlling the surface temperature of concrete by heat scanners: *a* – irradiation with the CO₂ gas ILGN-709 laser; *b* – irradiation with the CO₂ gas LGN-703 laser

To build the charts after the tests more accurately, the distance from the thermocouple to the center of the beam contact spot with the surface and the dimensions of other characteristic zones were measured (Table 1, [17]). The diameter of the laser beam spot, the diameter of the drying zone, as well as the size of the leaching zones of concrete, chemical dehydration reactions, the depth of the fused zone were measured.

of class C12/15 (1-2/7-8) at the age of 28 days decreased by 9.1 %. For other classes, this phenomenon was not registered. The registered increase in the strength of cubes at aging over 70 months amounted to 9–26 %.

Table 5

Results of the force and thermal force tests of samples from series I

Sample No.	Concrete class, C	W, (%)	$f_{cm,cube}$, (MPa) force/thermal force	Deviation from C, (%)	Age, day, at testing
1-2/7-8	12/15	2.72	19.14/19.25	-9.63/-9.11	30
	20/25	2.50	32.31/32.22	-0.06/-0.34	
	30/35	2.81	45.87/45.76	-0.78/-1.02	
3-4/9-10	12/15	0.80	21.18/21.08	$\pm 0.0/-0.47$	28
	20/25	0.92	32.33/32.30	0.0/-0.09	
	30/35	0.94	46.23/46.17	0.0/-0.13	
5-6/11-12	12/15	0	20.54/20.50	-3.02/-3.21	30
	20/25	0	31.75/31.91	-1.79/-1.3	
	30/35	0	46.02/45.85	-0.45/-0.82	
25-26/31-32	12/15	2.77	27.26/27.20	+28.7/+28.4	91
	20/25	2.54	33.15/33.10	+2.54/+2.38	
	30/35	3.02	46.89/46.93	+1.43/+8.56	
27-28/33-34	12/15	0.54	26.52/26.45	+25.2/+24.9	91
	20/25	0.66	32.93/33.19	+1.86/+2.66	
	30/35	0.43	47.10/47.05	+1.88/+1.77	
29-30/35-36	12/15	0	24.61/24.55	+16.2/+15.9	91
	20/25	0	32.28/32.29	-0.15/-0.12	
	30/35	0	46.21/46.02	-0.04/-0.45	
73-74/79-80	12/15	2.67	24.80/24.54	+17.1/+15.9	366
	20/25	2.63	34.99/35.00	+8.23/+8.26	
	30/35	2.85	48.11/47.93	+4.07/+3.68	
75-76/81-82	12/15	0.22	26.75/26.45	+26.3/+24.9	366
	20/25	0.48	35.01/34.86	+8.29/+7.82	
	30/35	0.51	48.79/48.67	+5.54/+5.28	
77-78/83-84	12/15	0	25.37/25.18	+19.8/+18.9	366
	20/25	0	32.84/32.91	+1.58/+1.79	
	30/35	0	47.82/47.83	+3.44/+3.46	
67-68/73-76	12/15	0	25.51/26.02	+20.4/+22.9	2,120
	12/15	0.4	26.22/26.03	+23.8/+22.9	
	12/15	3.04	25.65/25.47	+21.1/+20.3	

5. Results of the field study and their comparison with the numerical experiment

5.1. Results of studying the level of stresses in concrete in the zone of a laser irradiation

The results from determining the cube strength of samples at normal temperature and under the action of local laser heating are given in Tables 5–7. They contain cube strength values statistically averaged for two samples. Table 5 demonstrates that the strength of water-saturated concrete samples

The force and thermal force tests did not reveal the effect of laser radiation on reducing the cubic strength of concrete, regardless of its design class, moisture content, and tested age. An increase in cube strength was registered in the range of 20–25 % for samples from series I, 7–12 % for samples from series II, and 9–23 % for samples from series III. The nature of temperature distribution at the surface of a sample, discretely registered by a heat scanner, is shown in Fig. 3. It demonstrates that there is practically no temperature gradient on the contact spot; in the adjacent

areas, it is maximal. More than 30 % of the surface area of the cube is occupied by a region with temperatures of up to 50 °C, where one can completely neglect the influence of temperature.

Table 6

Results of the force and thermal force tests of samples from series II

Sample No.	Concrete class, C	W, (%)	$f_{cm,cubes}$ (MPa) force/thermal force	Deviation from C, (%)	Age, day, at testing
1-2/7-8	12/15	7.10	19.43/19.45	-0.41/-0.31	30
	20/25	2.34	31.97/32.06	-1.02/-0.74	
	30/35	1.86	45.12/45.00	+0.22/-0.04	
3-4/9-10	12/15	5.22	19.51/19.45	0.0/-0.31	28
	20/25	0.60	32.30/32.41	0.0/+0.34	
	30/35	0.38	45.02/44.88	0.0/-0.31	
5-6/11-12	12/15	0	19.49/19.29	-0.1/-1.13	30
	20/25	0	32.48/32.27	+0.56/-0.09	
	30/35	0	45.14/45.23	+0.27/+0.47	
25-26/31-32	12/15	7.13	20.07/20.31	+2.87/+4.1	90
	20/25	2.29	32.49/32.55	+0.59/+0.77	
	30/35	1.69	45.76/45.68	+1.64/+1.47	
27-28/33-34	12/15	4.84	20.10/21.06	+3.02/+7.94	90
	20/25	0.93	32.95/33.27	+2.01/+3.0	
	30/35	0.17	45.45/45.92	+0.95/+2.00	
29-30/35-36	12/15	0	19.73/19.56	+1.13/+0.26	90
	20/25	0	32.98/32.81	+2.1/+1.58	
	30/35	0	45.20/45.40	+0.4/+0.84	
73-74/79-80	12/15	7.32	21.29/21.93	+9.12/+12.4	370
	20/25	2.11	34.67/35.08	+7.3/+8.6	
	30/35	1.69	46.99/47.27	+4.38/+5.0	
75-76/81-82	12/15	4.84	21.64/21.36	+10.9/+9.48	370
	20/25	2.11	34.88/34.94	+7.99/+8.17	
	30/35	1.69	47.41/47.23	+5.31/+4.9	
77-78/83-84	12/15	0	21.15/21.37	+8.4/+9.53	370
	20/25	0	34.97/35.09	+8.27/+8.64	
	30/35	0	47.38/47.48	+2.24/+5.46	
67-68/73-76	20/25	0	35.60/34.59	+10.2/+6.99	2,130
	20/25	0.47	35.63/36.09	+10.3/+11.7	
	20/25	1.25	35.45/36.17	+9.8/+11.98	

Table 7

Results of the force and thermal force tests of samples from series III

Sample No.	Concrete class, C	W, (%)	$f_{cm,cubes}$ (MPa) force/thermal force	Deviation from C, (%)	Age, day, at testing
1-2/7-8	12/15	2.87	20.44/20.12	-2.25/-3.78	30
	20/25	2.38	34.18/34.35	-1.67/-1.18	
	30/35	2.01	47.33/47.53	-1.09/-0.67	
3-4/9-10	12/15	1.09	20.91/20.68	0.0/-1.1	28
	20/25	0.58	34.76/34.90	0.0/+0.4	
	30/35	0.56	47.85/47.78	0.0/-0.15	
5-6/11-12	12/15	0	20.03/19.98	-4.2/-4.45	30
	20/25	0	34.62/34.82	-0.4/+0.17	
	30/35	0	47.85/47.71	0.0/-0.29	
25-26/31-32	12/15	3.18	21.56/21.35	+3.1/+2.1	93
	20/25	4.37	34.95/35.00	+0.55/+0.69	
	30/35	3.86	48.09/47.99	+0.5/+0.29	
27-28/33-34	12/15	0.96	21.33/21.24	+2.0/+1.58	93
	20/25	1.87	35.06/35.16	+0.86/+1.15	
	30/35	0.32	48.11/48.02	+0.54/+0.36	
29-30/35-36	12/15	0	21.68/21.53	+3.68/+2.96	93
	20/25	0	34.77/35.15	+0.03/+1.12	
	30/35	0	48.05/47.89	+0.42/+0.08	

Continuation of Table 7

73-74/79-80	12/15	3.36	23.06/22.87	+10.28/+9.37	367
	20/25	4.24	36.16/36.27	+4.02/+4.34	
	30/35	3.40	49.30/49.19	+3.03/+2.8	
75-76/81-82	12/15	0.92	23.39/23.41	+11.9/+11.96	367
	20/25	0.08	36.12/35.83	+3.91/+3.1	
	30/35	0.32	49.15/48.96	+2.72/+2.3	
77-78/83-84	12/15	0	22.32/22.05	+6.74/+5.45	367
	20/25	0	35.57/35.43	+2.33/+1.93	
	30/35	0	48.93/48.64	+2.26/+1.65	
67-68/73-76	30/35	0	52.54/52.23	+9.80/+9.26	2,134
	30/35	0.41	55.97/55.38	+16.97/+15.7	
	30/35	1.26	58.61/58.74	+22.5/+22.76	

Fig. 4 shows the levels of K_p coefficient, registered by acoustic-emission control using the “ACEM” system. Its maximum value for the moment of contact of the laser beam with the concrete surface did not exceed $K_p=4.1-4.36$ (second 50) [18]. With further heating and reaching the tem-

peratures of 300–500 °C (second 90) at the contact of the concrete surface with a laser beam, the process of formation of macro cracks began when the walls of water-saturated pores of concrete were destroyed, which was also registered by acoustic and emission control.

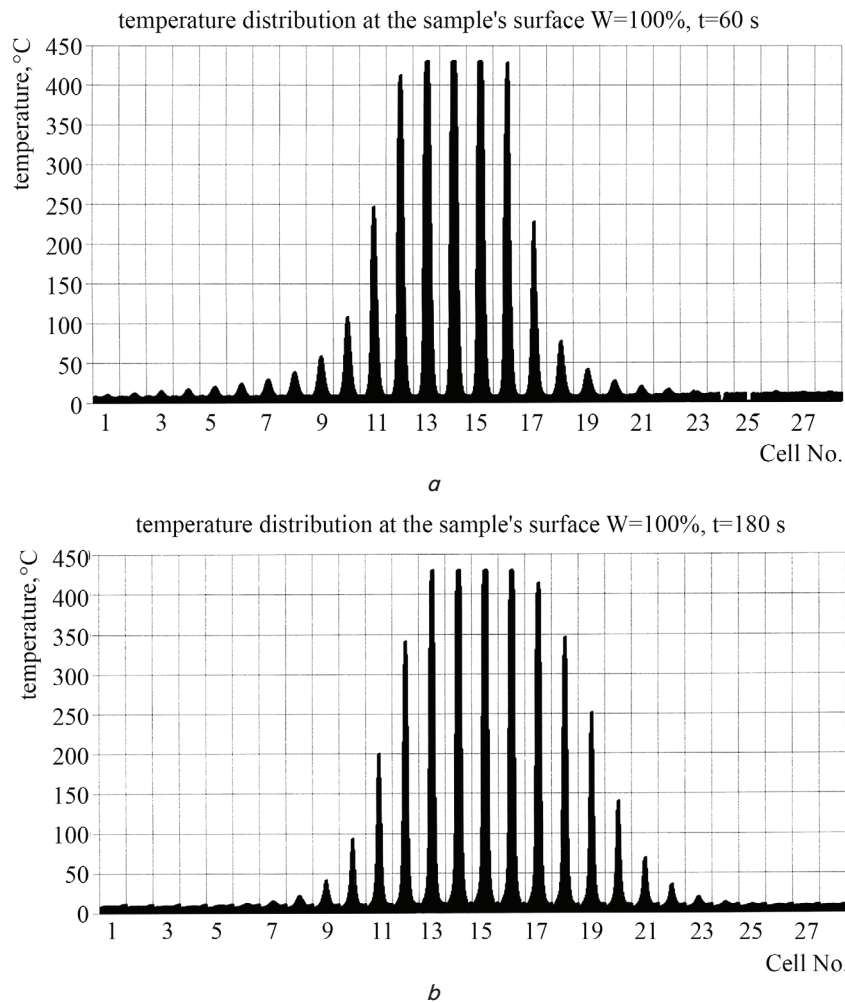


Fig. 3. Temperature distribution at the surface of a water-saturated sample (100 % of pores in concrete is filled with water) of concrete according to a heat scanner: *a* – 60 s of heating; *b* – 180 s of heating

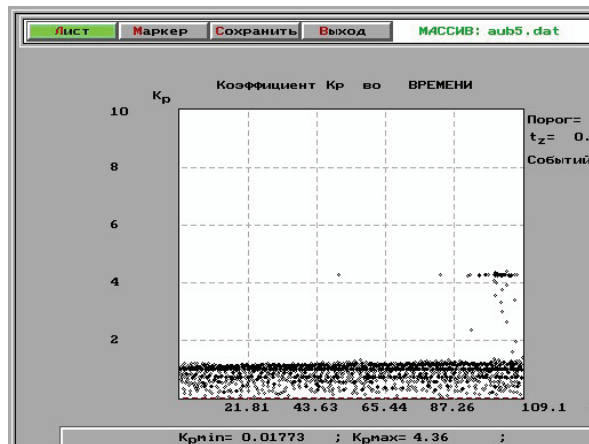


Fig. 4. Level of K_p coefficient for a concrete sample under local heating

When using the multichannel acoustic-emission control system “SAMOS-56” (Fig. 5), the phenomenon of a thermal shock (channel 1) and the formation of microcracks (channels 2–4) due to the single-axial compression during thermal force tests of cubes were also registered.

Control channels 2–4 show the process of formation of microcracks in concrete cubes with an increase in the compression load from 0 to 0.3 destructive and the cessation of their formation at aging at this level of load.

The maximum tangent stresses were 1.7 MPa, which corresponds to the coefficients $K_p=4.1–4.36$ [16], registered by the method of acoustic emission (Fig. 4).

Normal cracks were not registered.

The possibility of forming normal cracks in the contact area of the laser beam with concrete was shown by a numerical experiment at a rated radiation power of 500 W (task cube_50). At this radiation power, normal stresses in this zone increase to 4.5 MPa and above.

5.2. Results of studying the temperature fields and phase transitions

In the area of influence of laser radiation on water-saturated concrete, complex processes of interaction with the formation of a vitreous layer contact on the contact surface and underneath the intermediate porous layer were detected. The formation of an intermediate layer was facilitated by the constant evaporation of porous water from water-saturated concrete throughout the entire heating time. Water vapor under pressure contributed to the formation of a porous structure, the strength of which was sufficient both to maintain the vitreous layer on the surface and to preserve the adhesion of the porous layer to the concrete of the cube. Both layers, under the influence of water vapor pressure, were larger than the front face of the cube and were easily removed from the surface without the use of a mechanical tool.

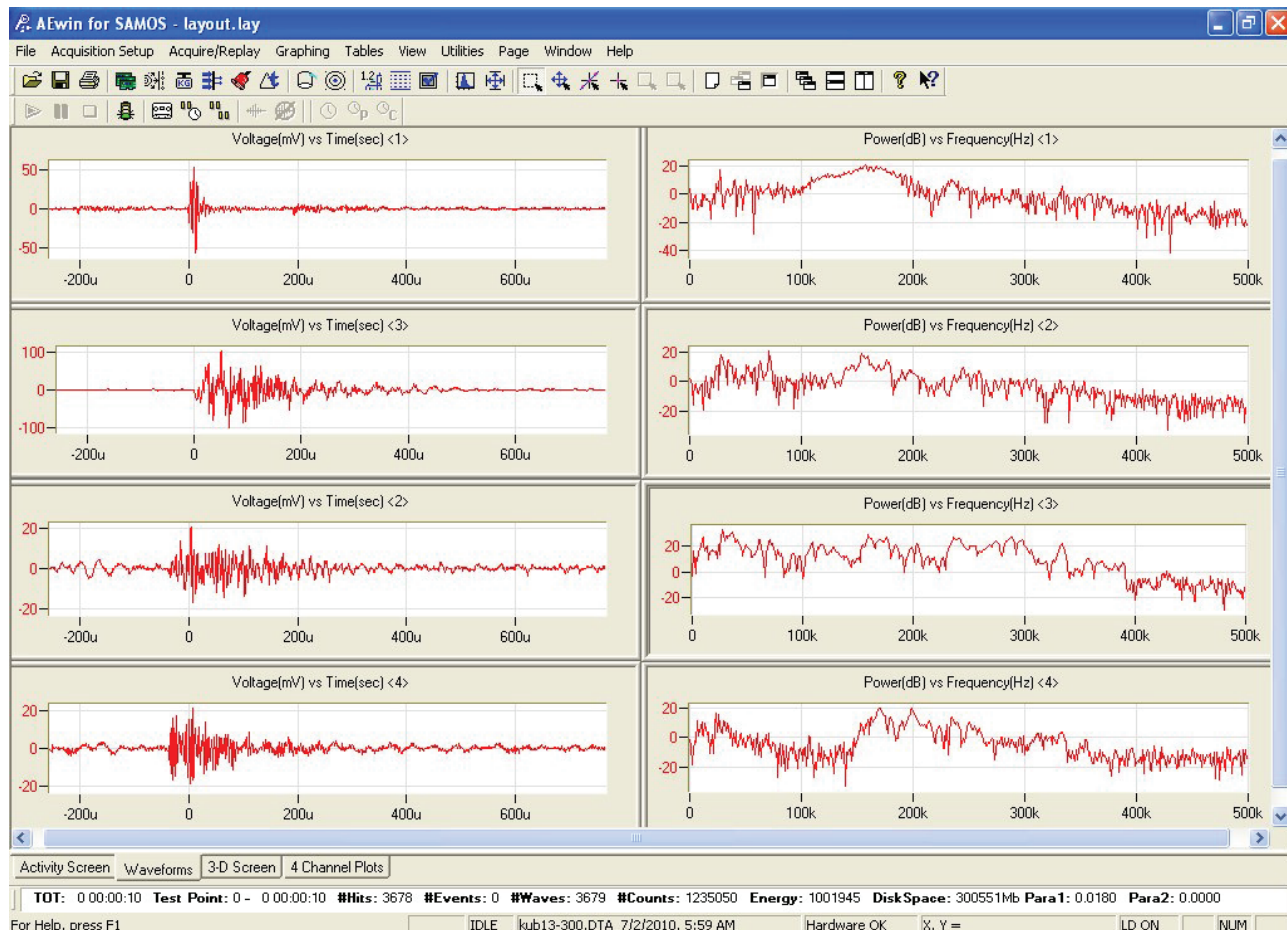


Fig. 5. The phenomenon of a thermal shock and the development of microcracks in concrete under the influence of laser radiation

The process of evaporation of moisture from the pores of water-saturated concrete continued throughout the entire experiment duration at atmospheric pressure. The dependence of the heat of evaporation on the boiling point must be taken into consideration according to the orthobulic curve for pressure $p=1.0 \text{ kg/cm}^2$ in the temperature range, which are registered in the contact spot for open pores. For closed pores, the pressure is taken equal to the calculated resistance of the concrete sample at stretching.

The average nature of the distribution of temperature over the surface and deep into the concrete samples obtained by the thermal scanner in the field experiment is shown in Fig. 6. The detection error was within the characteristics of the device $+50 \text{ }^\circ\text{C}$ in the temperature range $1,000\text{--}1,500 \text{ }^\circ\text{C}$, and $+10 \text{ }^\circ\text{C}$ at temperatures of up to $+800 \text{ }^\circ\text{C}$.

Temperature distribution over the surface in the depth of concrete (heating minute 5)

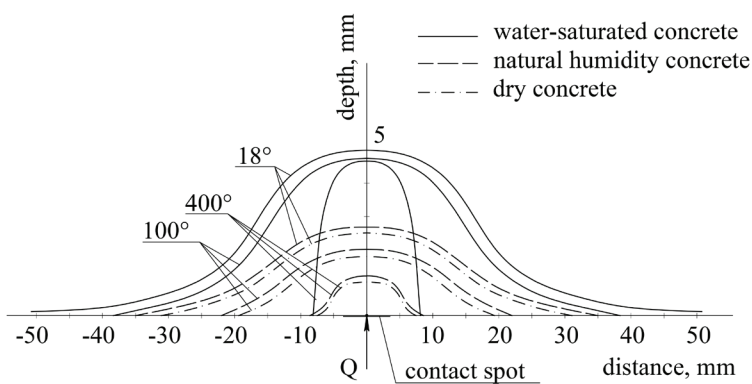


Fig. 6. Distribution of temperatures over the surface and deep into the concrete sample of the cube

Fig. 6 demonstrates that the surface area of concrete with a temperature above $50 \text{ }^\circ\text{C}$ did not exceed 20 cm^2 for dry concrete and concrete of natural humidity, and 64 cm^2 for water-saturated concrete. The maximum temperature on the surface of water-saturated concrete of $1,300\text{--}1,400 \text{ }^\circ\text{C}$ caused the appearance of plasma, burning on the surface of concrete, that is, 5 stages of interaction. For dry concrete and concrete of natural humidity, the second, third, and fourth stages of interaction were obtained at the same radiation power. The thresholds between the third and fifth stages of interaction of laser radiation with concrete are reduced by $10^3\text{--}10^4$ times. The depth of concrete heating also depends very much on its moisture content. For water-saturated concrete, the warming depth is on average 5 mm , and, for concretes with lower moisture content, does not exceed $2.5\text{--}2.6 \text{ mm}$. The volume of concrete heated above $50 \text{ }^\circ\text{C}$ did not exceed 2 cm^3 for dry concrete and concrete with natural humidity, and 10 cm^3 for water-saturated concrete.

5. 3. Computer model and its comparison with experimental study

The stationary problem was modeled taking into consideration results from the experimental study – the derived distribution of temperature over the surface and deep into the concrete cube for more than 100 samples of concrete at three levels of moisture content. At the same time, the distribution of temperatures along the depth and surface of

the samples was compared with the data acquired from the numerical experiment.

A concrete cube was simulated with three-dimensional elements No. 162 and No. 164 with a plate surface of heat exchange. A round spot of contact with the average diameter of a real spot in the shape of an oval with dimensions of $6\times 8 \text{ mm}$ was set, which was registered during experimental studies. Around the round contact spot, a physical body in the shape of a cube was added. The specified stiffnesses and mechanical boundary conditions corresponded to heavy concrete (dry, with natural humidity, and water-saturated) on the Portland cement. When modeling the thermal characteristics of the material, appropriate thermal conductivity coefficients were set out of three possible options for boundary temperature conditions:

- 1) on part of the contact boundary, the temperature $T=T_0$ is set;
- 2) on part of the contact boundary, the heat flow $Q=Q_0$ is set;
- 3) on part of the border, there is a heat exchange with the environment according to the law $Q+k(T-T_1)=0$, where k is the heat exchange coefficient, T_1 is the ambient temperature (adopted at $17\text{--}20 \text{ }^\circ\text{C}$ for experimental research). During modeling, the second variant of boundary conditions was selected, which is implemented similarly to the surface load since the rated power of the lasers used (30 W and 100 W) is known.

The vitreous layer was set in a computer model with a thermal conductivity coefficient of $0.11 \text{ W/m}\cdot^\circ\text{C}$ with a thickness of 1 mm . At the side surface of the layer where there is no direct contact with a laser beam, the third variant of temperature boundary conditions was used.

The dependence of the thermal conductivity coefficient of this layer on changes in temperature was neglected since at the interface of contact with an intermediate porous layer, thermal conductivity was considered constant. The intermediate porous layer with a thickness of 1 mm was modeled with foam concrete with a thermal conductivity coefficient of $0.08 \text{ W/m}\cdot^\circ\text{C}$. The thermal conductivity coefficient of concrete was set at the level of $1.5 \text{ W/m}\cdot^\circ\text{C}$ for concrete with a temperature not exceeding $100 \text{ }^\circ\text{C}$ under an intermediate porous layer of the foam concrete type.

The resulting temperatures at the fifth minute of heating and from a numerical experiment for the dynamic equilibrium of temperature fields are given in Table 8; for the depth of the concrete sample cube – in Table 9, for characteristic points (nodes of volumetric finite elements).

In Table 9, $q=Q/A_c$, where $A_c\approx 38 \text{ mm}^2$ is the average contact area of the laser beam with the surface of the sample. $Q=100 \text{ W}$ is the rated power of laser radiation.

The average temperature distribution over the surface of concrete cube samples for the rated power of the laser 100 W (problem “cube_10”) is shown in Fig. 7, 500 W (problem “cube_50”) – in Fig. 8.

The deformed model of the cube under temperature loads confirms the protrusion of vitreous and porous layers beyond the front face of the cube, registered in the field experiment.

Analysis of the level of normal and tangent stresses in the heated volume of concrete sample cube was carried out for the numerical experiments “cube_10” and “cube_27” (the rated

radiation power is 100 W and 270 W). These problems were chosen for analysis because the resulting temperature fields are the closest to the temperature fields registered in the field experiments on minute 5 of heating when they are stabilized.

struction of pore walls were detected by acoustic-emission control during the experimental study (level $K_p > 4$).

Computer simulation confirmed the absence of normal microcracks (level $K_p < 6$) in the concrete of cubes due to the hoop effect of point laser heating for 5 minutes. In the computer simulation, the volume of heated concrete did not exceed 1–2 % of the sample volume, which corresponds to the values obtained in a full-time experiment.

Table 8

Distribution of temperatures on the surface of samples, °C

Distance from the center of a heated point, mm	Problem title					
	cube_100	cube_77	cube_50	cube_27	cube_10	field experiment*
0	6,931	5,336	3,476	1,898	1,526	1,350±50**
1.1	6,798	5,234	3,409	1,863	1,496	1,350±50**
2.3	6,354	4,892	3,187	1,743	1,400	1,350±50**
3.5	6,206	3,779	3,113	1,704	1,368	1,350±50**
4.7	2,431	1,874	1,225	673	503	750
5.8	1,828	1,411	924	509	380	570
7.0	1,439	1,112	730	403	300	445
9.0	1,075	831	547	304	227	338
11.0	863	669	442	246	185	269
13.0	724	562	372	209	158	230
15.0	627	487	323	183	139	201
20.0	465	362	242	140	107	155
25.0	378	295	199	116	90	132
30.0	324	254	172	102	79	118
35.0	288	226	154	92	72	106
40.0	263	207	142	85	67	96
45.0	247	194	133	81	64	87
50.0	237	187	128	78	62	79

Note: * – averaged from 24 water-saturated samples of series III; ** – according to the visual pyrometer “Promin”

Solving a stationary problem of thermal elasticity in computer simulation of the process of interaction of the laser beam with concrete makes it possible to describe the temperature fields in concrete in general. It is possible to determine the stresses in concrete in the zone of laser radiation exposure for the contact zone of the beam with concrete and the area outside the zone.

Comparing the results from the natural physical [17] and numerical experiments reveals (Table 8) that the percentage of radiation power spent on heating concrete depends on the surface temperature. In the spot of contact with a temperature exceeding 1,300 °C, this percentage is not more than 8–10 %, and, outside it, increases to 24–25 %. In thermal force tests at the joint action of temperature in the contact spot of 1,300–1,400 °C, which corresponds to the results from a numerical experiment for the problem cube_10, and at three levels of single-axial compression load, the same results were obtained. Outside the contact spot, the surface temperature of the cubes obtained in a full-time experiment corresponded to that for the problem cube_27 obtained in a numerical experiment. That is, the levels of energy transmission in the contact spot for heating 100 W; 77 W; 50 W; 27 W; 10 W from the beam correspond to the output power of the laser of 1,000 W; 770 W; 500 W; 270 W; 100 W, respectively (Table 8). The increase in the share of power for heating outside the contact spot is associated with the presence of ray radiation from the surface of the plasma, as well as the absorption of heat of secondary radiation by water vapor. Such features of the process of spot heating of concrete under the action of laser radiation cannot be taken into consideration when solving a stationary thermal conductivity problem. The same results were obtained when comparing the temperatures in the depth of concrete (Table 9). The nature of the temperature distribution on the surface of the sample,

Table 9

Distribution of temperatures in the sample thickness, °C

Problem title	q, W/mm ²	Measurement point depth, mm				
		1.0	2.0	3.0	4.0	5.0
cube_100	2.6	7,132	2,481	2,198	1,694	1,488
cube_77	2.0	5,490	1,913	1,695	1,486	1,308
cube_50	1.3	3,576	1,251	1,109	973	857
cube_27	0.7	1,952	687	609	535	472
cube_10	0.26	1,526	443	412	373	336
exp*	2.6	1,350±50**	658	548	465	400

Note: * – averaged from 24 water-saturated samples of series III; ** – according to the visual pyrometer “Promin”

The gradients of temperature over the surface of concrete cubes obtained according to the heat scanner and pyrometer are consistent with those obtained in the numerical experiment for the above problems cube_10 and cube_27; the deviation does not exceed 10–12 %.

At the same time, it is necessary to set 10 % and 25 % of the rated power of laser radiation, respectively, for the processes of concrete heating.

In computer simulation, the formation of macro cracks due to the tangent stresses created by temperature gradient and pressure of water vapor has been confirmed. Cracks in the pores of water-saturated concrete samples and the de-

struction of pore walls were detected by acoustic-emission control during the experimental study (level $K_p > 4$). Computer simulation confirmed the absence of normal microcracks (level $K_p < 6$) in the concrete of cubes due to the hoop effect of point laser heating for 5 minutes. In the computer simulation, the volume of heated concrete did not exceed 1–2 % of the sample volume, which corresponds to the values obtained in a full-time experiment. Solving a stationary problem of thermal elasticity in computer simulation of the process of interaction of the laser beam with concrete makes it possible to describe the temperature fields in concrete in general. It is possible to determine the stresses in concrete in the zone of laser radiation exposure for the contact zone of the beam with concrete and the area outside the zone. Comparing the results from the natural physical [17] and numerical experiments reveals (Table 8) that the percentage of radiation power spent on heating concrete depends on the surface temperature. In the spot of contact with a temperature exceeding 1,300 °C, this percentage is not more than 8–10 %, and, outside it, increases to 24–25 %. In thermal force tests at the joint action of temperature in the contact spot of 1,300–1,400 °C, which corresponds to the results from a numerical experiment for the problem cube_10, and at three levels of single-axial compression load, the same results were obtained. Outside the contact spot, the surface temperature of the cubes obtained in a full-time experiment corresponded to that for the problem cube_27 obtained in a numerical experiment. That is, the levels of energy transmission in the contact spot for heating 100 W; 77 W; 50 W; 27 W; 10 W from the beam correspond to the output power of the laser of 1,000 W; 770 W; 500 W; 270 W; 100 W, respectively (Table 8). The increase in the share of power for heating outside the contact spot is associated with the presence of ray radiation from the surface of the plasma, as well as the absorption of heat of secondary radiation by water vapor. Such features of the process of spot heating of concrete under the action of laser radiation cannot be taken into consideration when solving a stationary thermal conductivity problem. The same results were obtained when comparing the temperatures in the depth of concrete (Table 9). The nature of the temperature distribution on the surface of the sample, obtained in a numerical experiment, is well consistent with those obtained by a heat scanner in the full-time experiment (Fig. 3). The deviation of the heat scanner’s readings and data from the numerical experiment did not exceed 9–12 % during the entire period of the experiment. Both in the full-time and numerical experiments, more than 30 % of the surface area of the cube is occupied by a zone with temperatures of up to 50 °C where one can completely neglect their effect on strength. For all studied classes of concrete, the levels of compression stress, and moisture content levels, no influence of the local temperature load on strength was detected.

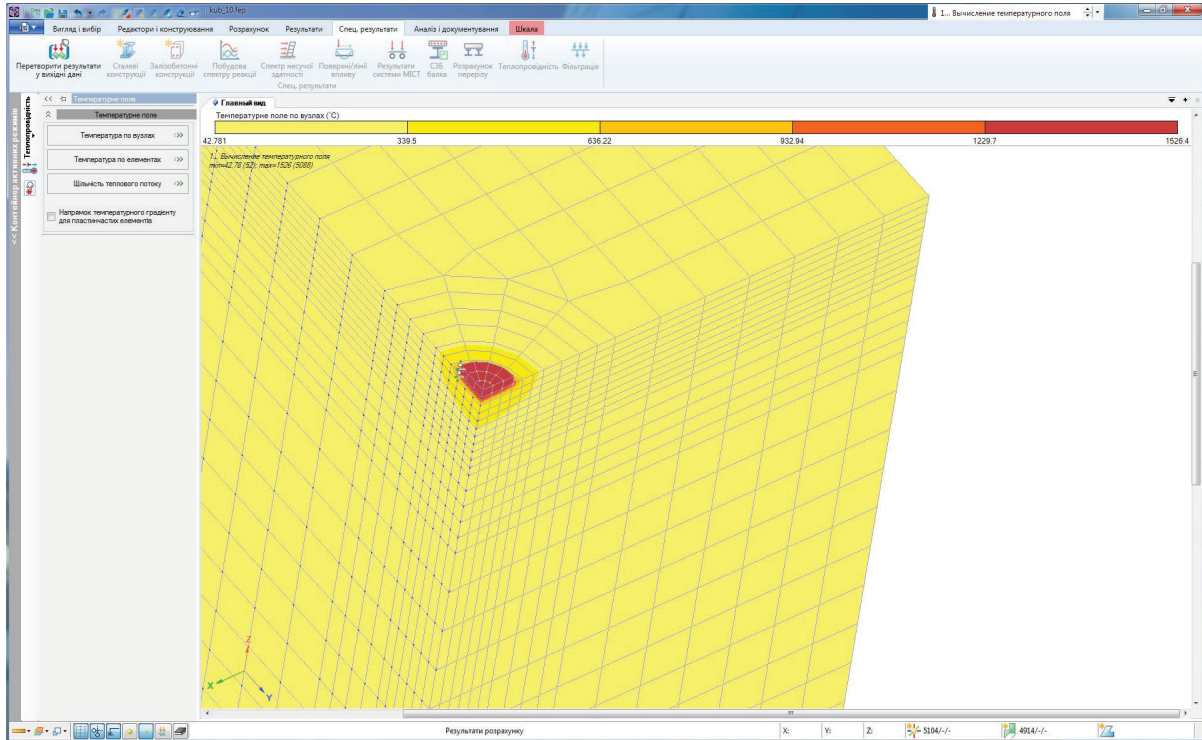


Fig. 7. Distribution of temperatures over the surface and in the volume of a water-saturated concrete cube, problem “cube_10”, the rated power of the laser is 100 W

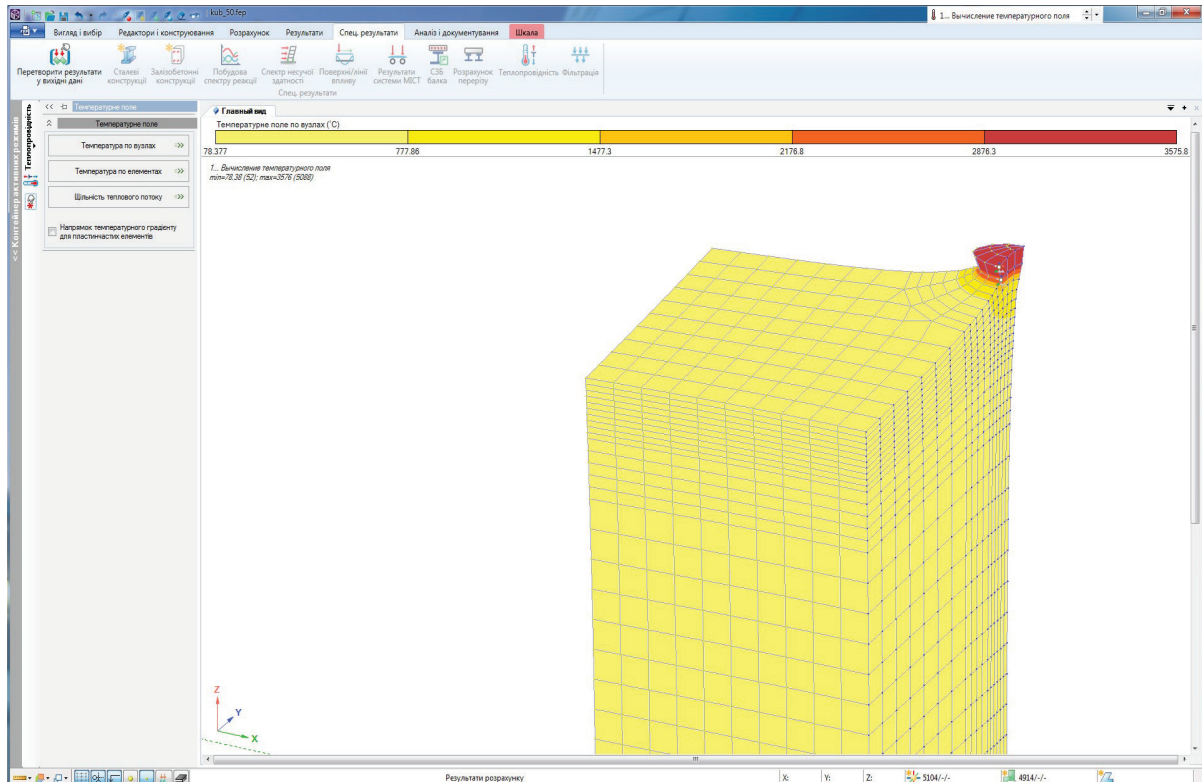


Fig. 8. Distribution of temperatures over the surface and in the volume of a water-saturated concrete cube, problem “cube_50”, the rated power of the laser is 500 W

5. 4. Application of laser technologies for the machining of concrete surfaces

At a radiation power of 10^2 W/cm^2 , the concrete surface warms up to temperatures of 300–450 °C in 25–30 seconds.

That makes it possible to remove any organic contaminants from the surface of concrete without damaging its structure. Moving a beam at a speed of 0.5–2.0 cm/s makes it possible to machine larger areas and surfaces that are difficult to

clean with other equipment. To this end, one can use lasers with a rated power of 30 W. Processing deep into concrete is possible with its water saturation using lasers with a rated capacity above 300 W. It is possible to reduce the power to safe, if necessary, only surface treatment by increasing the area of contact spot by optical means. In this case, every 20–30 s, it is necessary to remove from the surface the vitreous and porous layers to obtain contact of the laser beam with deeper layers of concrete. Dry concrete surfaces are poorly treated, even at higher radiation power. Such concrete has high protective properties under the loads due to local laser heating. Research in this area must be continued using lasers of greater rated power.

6. Discussion of results of studying the interaction between a local laser temperature load and heavy concrete

The study that involved lasers of two levels of power has made it possible to clarify the thresholds between the stages of interaction of laser radiation with the surface of heavy concrete. Significant compaction and a decrease in the levels of thresholds were detected, by 10^3 – 10^4 times compared to metals, especially for water-saturated concrete. When investigating the effect of concrete moisture content on this nature of interaction, the phenomenon of plasma combustion at the contact spot (the fifth stage of interaction) was registered. At the same time, the formation of vitreous and intermediate porous layers on the contact spot area was registered. The porous layer formed under the influence of water evaporation, unlike the CO_2 effect reported in work [17], is strong enough to serve as additional thermal insulation, which slows down the deep warming up of concrete. However, the detected difference in temperature fields in the depth of dry and water-saturated samples is less than one might expect (Fig. 6), precisely due to the presence of intermediate layers. Drying concrete can significantly increase the protective properties of the material (warming depth is reduced 2 times compared to water-saturated concrete). The best protective properties of dry concrete and concrete with natural humidity, compared to water-saturated concrete, are explained by much lower thermal conductivity coefficients and the presence of a vitreous layer, which enhances the reflective properties of the surface. The absence of normal macrocracks in concrete is explained by the levels of K_p , obtained in the process of acoustic-emission control (Fig. 4), and the hoop effect due to the insignificant volume of heated concrete compared to the sample volume. No decrease in cube strength was registered in the experimental thermal force studies due to a very insignificant volume of heated concrete and melting zone and erosion, which, for the experiment duration of 5 minutes, amounted to no more than 1%. The method of acoustic-emission control (Fig. 5) has made it possible to record the processes of microcracking during thermal force tests and confirm their absence under the action of laser heating.

Comparing results from the experiments and a computer model (Table 8) indicates the possibility of using the developed computer model in the statement of a stationary thermal elasticity problem for calculating temperature fields and changes in the stressed-strained state of heavy concrete in the area of laser radiation. Almost the same temperature was registered over the entire area of the contact spot (Fig. 3),

the formation of vitreous and porous layers of material on it can be explained by the uniform distribution of thermal energy over the area of the beam. No impact of concrete strength and initial stress level was detected at their joint action with temperature load on the final strength of concrete at compression (Tables 5–7). That makes it possible to more reasonably approach the design of reinforced concrete protective structures. It becomes possible to more accurately assess the impact of the local temperature load on reinforced concrete structures of enterprises executing high-temperature technological processes. Taking into consideration various shares of the thermal energy of radiation spent on heating concrete in the contact zone and beyond is a non-stationary problem that has not been solved. Therefore, when designing, discrete solutions of a stationary problem can be used for (10% for the contact zone and 27% out of area). A numerical experiment showed that at a rated radiation power of at least 500 W (Fig. 8), normal stresses in this zone increase to 4.5 MPa and above, and therefore normal cracks are formed in this zone of laser beam contact with concrete. This greatly accelerates the process of concrete erosion and the possibility of its processing in depth, as registered in the operation [12] when using a laser with a capacity of 1.6 kW. Removing vitreous and porous layers with a jet of water or compressed air makes it possible to improve the processing of concrete surfaces regardless of the direction of the laser beam, unlike the upright direction offered in work [12]. More powerful lasers should be used than during the experiments reported here (above 500 W), which would make it possible to deeply machine surfaces and form holes in cement-based materials (solutions, concretes, asbestos cement, etc.).

The obtained results provide an opportunity to continue studying the possibility of deeper treatment of concrete surfaces, as well as constructing new computer models of these processes.

7. Conclusions

1. The stressed-strained state of concrete in the zone of interaction with laser radiation of rated power of 100–1,000 W is characterized by the existence of tangent stresses of 0.2–1.7 MPa. Stresses at the level of 1.6–1.7 MPa were achieved at a rated radiation power of 100 W; they lead to the destruction of the walls of pores and erosion. The vitreous and porous layers up to 2 mm thick, formed under the influence of laser radiation and plasma combustion at the surface of water-saturated concrete, reduce the temperature gradients and stresses in deeper layers of concrete and improve its protective properties. Such an impact did not lead to a decrease in the strength of concrete at compression, regardless of the level of stresses during thermal force tests.

2. A significant (destructive at maximum temperatures of up to 1,400 °C) influence of laser radiation on the structure of the concrete surface at the place of heating has been confirmed. Plasma combustion (stage 5 of interaction) was detected on the surface of contact with water-saturated concrete. Dried concrete and concrete of natural humidity showed high protective properties under such a high-temperature effect on the surface (stage 2 of interaction at a rated radiation power of 30 W, stage 4 at a power of 100 W). A significant decrease in the thresholds between the stages of interaction of laser radiation with concrete compared to the

thresholds for metals was detected (the thresholds between the third and fifth stages were reduced by 10^3 – 10^4 times).

3. The use of a stationary thermal elasticity problem in a numerical experiment makes it possible to reliably describe the temperature fields in concrete in contact with a laser beam. It becomes possible to discretely determine the stresses in concrete in the zone of laser radiation exposure for the contact zone of the beam with concrete and the area outside the zone.

In this case, it is necessary to set 10 % and 25 % of the rated power of laser radiation, respectively, for the processes of concrete heating.

In computer simulation, the formation of macro cracks was confirmed due to the tangent stresses created by a temperature gradient and the pressure of water vapor in the pores of water-saturated concrete samples, as well as their destruction, which were detected by acoustic-emission control during the experimental study (level $K_p > 4$).

Computer simulation has confirmed the absence of normal microcracks (level $K_p < 6$) in the concrete of cubes due to the hoop effect of point laser heating for 5 minutes. In computer modeling, the volume of heated concrete did not

exceed 1–2 % of the sample volume, which corresponds to the values obtained in a full-time experiment.

4. Laser technologies with a moving beam of at least 10^3 W/cm² could be used to machine (clean) the concrete surface. Depending on the rated power of laser radiation, the effective cleaning of the concrete surface from organic, paint, and other types of contamination is ensured at the rate of movement of the beam of 0.5–2 mm/s (surface temperature, 100–300 °C).

Machining the depth of concrete with a stationary beam is possible at periodic (every 25–30 s) removal of a layer of vitreous mass and a porous layer from the contact surface mechanically (air or water under pressure).

Acknowledgments (if any)

I would like to express my gratitude to Professor P. Y. Stakhyra, engineer V. O. Dolnikov, engineer O. B. Futalo, senior researcher E. V. Hlavatsky for their assistance in conducting experiments and contributing to this study.

References

- Baharev, S., Mirkin, L. I., Shesterikov, S. A. et. al. (1988). *Struktura i prochnost' materialov pri lazernykh vozdeystviyakh*. Moscow: Izd-vo Mosk. un-ta, 224.
- Anishchenko, L. M., Lavrenyuk, S. Yu. (1986). *Matematicheskie osnovy proektirovaniya vysokotemperaturnykh tekhnologicheskikh protsessov*. Moscow: Nauka, 77.
- Wignarajan, S. (1999). New horizons for high-power lasers: applications in civil engineering. *Proceeding SPIE*, 3887-01, 34–44.
- Uglov, A. A., Smurov, I. Yu., Lashin, A. M., Gus'kov, A. G. (1991). *Modelirovanie teplofizicheskikh protsessov impul'snogo lazernogo vozdeystviya na metally*. Moscow: Nauka, 288.
- Rozniakowski, K. (2001). *Zastosowanie promieniowania laserowego w badaniach i modyfikacji właściwości materiałów budowlanych*. Studia z zakresu inżynierii NR 50. Warszawa-Lódź, 200.
- Romanowska, A., Jablonski, M. (2001). *Kompozyt gipsowy o podwyższonej akumulacji ciepła*. Studia z zakresu inżynierii NR 50. Warszawa-Lódź, 102.
- Gawin D., Kośny J., Wilkes, K. (2005). *Wpływ zawartości wilgoci na dokładność pomiaru współczynnika przewodzenia ciepła betonu komórkowego metodą stacjonarną*. Polska academia nauk. Studia z zakresu inżynierii NR 50. Warszawa-Lódź, 88.
- Kamata, H., Mimori, T., Tachiwa, M., Sugimoto, K. (1996). *New Applications of Lasers to Architecture and Civil Engineering. Study on Methods for Decontaminating Concrete Surface by Laser Treatment*. *The Review of Laser Engineering*, 24 (2), 182–190. doi: <https://doi.org/10.2184/laj.24.182>
- Hamasaki, M. (1987). *Experimental cutting of biological shield concrete using laser*. Proc. International Symposium on Laser Processing. Tokio.
- Stashuk, P. M. (2001). *Vyvchennia kinetyky protsesiv trishchynoutvorennia metodom akustychnoi emisii*. *Visnyk Derzhavnoho universytetu "Lvivska politekhnika" Teoriya ta praktyka budivnytstva*, 178–184.
- Filonenko, S. F. (2000). *Analiz kinetiki razvitiya protsessov razrusheniya metodom akusticheskoy emissii*. *Mezhdunarodnaya nauchnaya konferentsiya "Sinergetika 2000. Samoorganizuyushchiesya protsessy v sistemah i tekhnologiyah"*. Komsomol'sk-na-Amure, 94–97.
- Long, N. P., Daido, H., Yamada, T., Nishimura, A., Hasegawa, N., & Kawachi, T. (2017). *Experimental characterization of concrete removal by high-power quasicontinuous wave fiber laser irradiation*. *Journal of Laser Applications*, 29 (4), 041501. doi: <https://doi.org/10.2351/1.5008326>
- Lawrence, J., Li, L. *High power diode laser surface glazing of concrete*. CORE. Available at: <https://core.ac.uk/download/pdf/53233.pdf>
- Sakai, Y., Sikombe, I., Watanabe, K., Inoue, H. (2019). *Microscopic Change in Hardened Cement Paste due to High-Speed Impact*. *Journal of Advanced Concrete Technology*, 17 (9), 518–525. doi: <https://doi.org/10.3151/jact.17.518>
- DSTU B V.2.7-214:2009. *Building material. Concretes. Methods for strength determination using reference specimens* (2010). Kyiv, 43.
- DSTU B V.2.7-170:2008. *Building materials. Concretes. Methods of determination of middle density, moisture content, water absorptions porosity and watertightness*. Kyiv.
- Karhut, I. I. (2019). *Influence of laser radiation on heavy concrete*. *Resource-saving materials, structures, buildings and structures*, 37, 35–47. doi: <https://doi.org/10.31713/budres.v0i37.311>
- Karkhut, I. I., Bula, S. S., Soroka, Ya. V. (2007). *Rozpodil temperatury v obiami betonu pry diyi teplovoho udaru, yak vydu mistsevoho nahrivu*. VII Mizhnarodnyi sympozium «Mekhanika ta fizyka ruinuвання budivnykh materialiv i konstruktsiy». Kyiv, 7, 191–197.